

# The Crack Initiation and Propagation in threshold regime and S-N curves of High Strength Spring Steels

N Gubelj<sup>1</sup>, J Predan<sup>1</sup>, B Senčič<sup>2</sup> and M D Chapetti<sup>3</sup>

<sup>1</sup> University of Maribor, Faculty of Mech. Eng., Maribor, Slovenia

<sup>2</sup> Štore Steel d.o.o., Steelwork company, Štore, Slovenia

<sup>3</sup> Laboratory of Experimental Mechanics, INTEMA, CONICET – University of Mar del Plata. Juan B. Justo 4302, Argentina

E-mail: [nenad.gubelj@um.si](mailto:nenad.gubelj@um.si)

**Abstract.** An integrated fracture mechanics approach is proposed to account for the estimation of the fatigue resistance of component. Applications, estimations and results showed very good agreements with experimental results. The model is simple to apply, accounts for the main geometrical, mechanical and material parameters that define the fatigue resistance, and allows accurate predictions. It offers a change in design philosophy: It could be used for design, while simultaneously dealing with crack propagation thresholds. Furthermore, it allows quantification of the material defect sensitivity. In the case of the set of fatigue tests carried out by rotational bending of specimens without residual stresses, the estimated results showed good agreement and that an initial crack length of 0.5 mm can conservatively explain experimental data. In the case of fatigue tests carried out on the springs at their final condition with bending at  $R = 0.1$  our data shows the influence of compressive residual stresses on fatigue strength. Results also showed that the procedures allow us to analyze the different combinations of initial crack length and residual stress levels, and how much the fatigue resistance can change by changing that configuration. For this set of tests, the fatigue resistance estimated for an initial crack length equal to 0.35 mm, can explain all testing data observed for the springs.

## 1. Introduction

Spring leaves usually fail by surface or subsurface induced fatigue failure from an inclusion, which size is relatively large in leaf spring. The fatigue crack growth area is often less than  $1\text{mm}^2$ . Usually, spring leaves fail by subsurface induced failure in the vicinity of an inclusion, as is shown in Fig. 1, during fatigue test. The initiation location depends of different parameters associated with the fatigue mechanism that gives rise to a crack, and then it is related with the weakest configuration of material resistance, inclusion size (the inclusion acts as a concentrator), residual stresses and loading. Few investigations of residual stress effect and inclusion size on fatigue failure in very high cycle regime has been performed by Shiozawa and co-workers [1, 2, 3]. They show that in case of rotating bending usually fatigue crack appear from surface inclusion induced failure mode, where compressive stress relaxed and decreased at an early stage of fatigue cycling. Therefore, compress residual stress on the surface are also not stable and uniform for fatigue lifetime prediction, as well. It is known that negative loading R ratio corresponds to negative value of minimum stress intensity factor  $K_{\min}$  and shift fatigue threshold  $\Delta K_{\text{th}}$  to higher values. The goal of producer is induced compress residual stresses in layer of leaf exposed to tension applied stress. During the crack initiation period fatigue crack develop during the first loading cycles, but depending on the magnitude of load become



quiescent for some time before they eventually succeed in crossing existing barrier as is shown in Fig. 2. The microstructural barrier is the grain boundary, where micro-crack can be retarded or stop. The stress range that leads to a very long or an infinite fatigue lifetime is called fatigue limit  $\Delta\sigma_{eR}$ . In principle the fatigue limit stress range is measured on smooth specimens and can remain constant even when very short crack (smaller than grain size) are present, as is schematically shown in so-called Kitagawa-Takahashi diagram in Fig. 3 [4]. In this approach the difference between the total applied driving force and the material threshold for crack propagation defines the effective driving force applied to the crack. The initial crack length is given by the position of the strongest microstructural barrier if the material were free of cracks or crack like flaws, or by the greatest defects that acts as a fatigue initiator.



Fig. 1. Leaf spring bar section with inclusion around 0.4 mm under surface at distance 0.8 mm

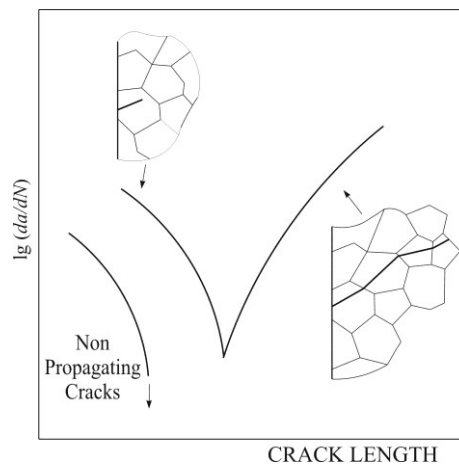


Fig. 2 Schematic view of retarded crack growing

The minimum threshold for fatigue crack propagation is associated to the microstructural barrier that defines the plain fatigue limit and represents the microstructural threshold for crack propagation, as [5]:

$$\Delta K_{dR} = Y \cdot \Delta\sigma_{eR} \sqrt{\pi \cdot d} \quad (1)$$

where  $Y$  is the geometrical correction factor. In most cases the nucleated microstructurally short surface cracks are considered semicircular, and the value of  $Y$  would then be 0.65[15]. Because the plain fatigue limit depends on the stress ratio  $R$ , the microstructural threshold also does. The value of  $d$  is usually given by the microstructural characteristic dimension, as inclusion or grain size, e.g. for

the steel in as-delivered condition  $d = 10 \mu\text{m}$ . The grain size in as-delivered condition is consequence of a conventional casting process. The fine grain was obtained by heating to the austenitizing temperature of  $+870^\circ\text{C}$  and gas quenched a temperature of  $+60^\circ\text{C}$ , and then tempered for 1 h at  $+475^\circ\text{C}$ . The inclusion size was reduced by Q+T process of refined spring steel, to size less than  $5 \mu\text{m}$ . However, some inclusions of size more than  $0.4$  was revealed under surface, representing critical locations for crack initiation.

A total extrinsic threshold to crack propagation,  $\Delta K_{\text{CR}}$ , is then defined by the difference between the crack propagation threshold for long cracks,  $\Delta K_{\text{thR}}$ , and the microstructural threshold,  $\Delta K_{\text{dR}}$  [5-8]. The development of the extrinsic component is considered to be exponential and a development parameter  $k$  is estimated as a function of the same microstructural and mechanical parameter used to define the material threshold for crack propagation. The material threshold for crack propagation as a function of the crack length,  $\Delta K_{\text{th}}$ , is then defined as [5]:

$$(2) \quad \Delta K_{\text{th}} = \Delta K_{\text{dR}} + (\Delta K_{\text{thR}} - \Delta K_{\text{dR}}) \left[ 1 - e^{-k(a-d)} \right] = Y \Delta \sigma_{\text{th}} \sqrt{\pi a} \quad a \geq d$$

Where the parameter  $k$  is given by:

$$k = \frac{1}{4d} \left( \frac{\Delta K_{\text{dR}}}{\Delta K_{\text{thR}} - \Delta K_{\text{dR}}} \right) \quad (3)$$

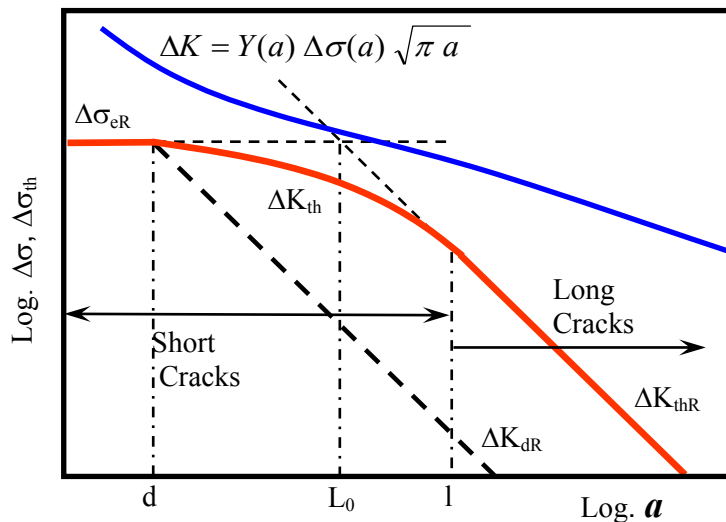


Fig. 3. Threshold curve concept in terms of the stress intensity factor range

Compressive residual stresses are produced by cold reverse bending. These compress residual stresses will act to protect the spring against its tensile service loads. High surface compressive residual stress value is produced by shot-peening. Shot-peening prevent fatigue crack propagation from the surface of bending loaded spring leaf. Properly done shot-peening generates high compress residual stresses and the fatigue crack process starts from the inclusion under the surface. However, producers of spring steel are faced with keeping constant quality of spring. Usually, production of steel has led to a reduction of the inclusion size in order to improve fatigue strength of steel. Springs after heat treatment are subjected to prestressing by cold reverse bending. Figure 4 shows an usual prestressing applied to truck springs. It is then placed in a fixture that loads it exactly as it will be loaded in service but at a level above tensile yield strength. When the load is released, it springs back to a new shape, which is that desired for assembly. However, the elastic recovery has now placed the material that yielded into a residual-stress state, which will be in the opposite (compressive) direction from that of

the applied load. Therefore these compress residual stresses will act to protect the spring against its tensile service loads. Properly shot-peening springs can have their fatigue strengths increased to the point that they will fail by yielding instead of failing by fatigue [9]. The two treatments are additive on the upper surface in this case, affording greater protection against tensile stresses in fatigue. Note that if the spring were reversely loaded in service up to yielding, the beneficial compressive stress could be relieved compromising the fatigue life of the spring.

The aim of this study is to clarify the effect of residual stress in spring under surface layers and estimate fatigue life time, as interaction between inclusion size and residual stress under surface. The analysis is carried out by using a fracture mechanic approach and dealing with the resistance curve concept, quantifying the applied driving force and the resistance for different configurations of residual stresses and inclusion sizes.

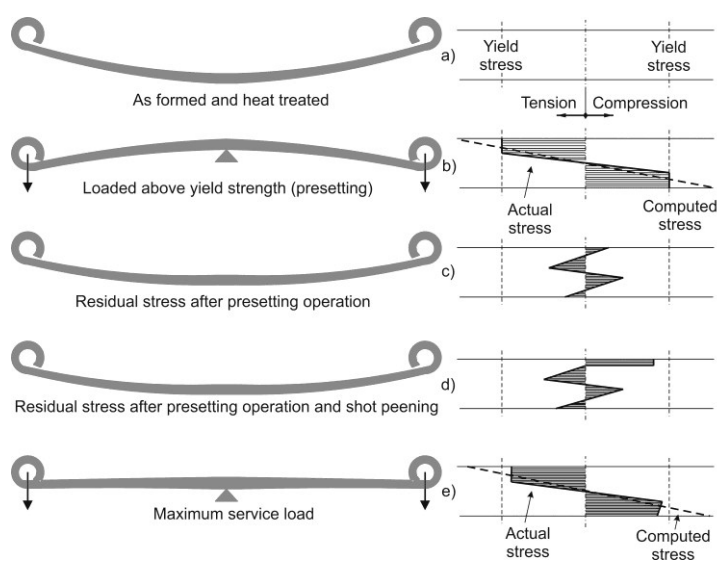


Fig. 4. Residual stresses profile from prestressing and shot-peening a leaf spring [9]

## 2. Material properties and residual stress measurements

Spring steel is delivered to spring producer in hot rolled condition as ferrite-perlite microstructure, with average grain size  $d=10\ \mu\text{m}$  and average hardness  $430\ \text{HV}$  ( $42\pm 2\ \text{HRc}$ ). Its tensile mechanical properties of steel as delivered condition are  $R_{p0.2}=1050\ \text{MPa}$  and ultimate tensile strength  $\sigma_u=1270\ \text{MPa}$  in average [10,11]. The spring's manufacturer performs hot rolling, hot bending, eye making and heat treatment. The goal of heat treatment is to achieve fine microstructure of tempered martensite with average grain size  $d=5\ \mu\text{m}$  and average hardness  $590\ \text{HV}$  ( $52\pm 2\ \text{HRc}$ ). Tensile mechanical properties of the steel as delivered conditions are  $R_{p0.2}=1580\ \text{MPa}$  and ultimate tensile strength  $\sigma_u=1670\ \text{MPa}$ . Inclusions are usually MnS, alumo-silicates and TiN. The size of inclusions varies between  $35\ \mu\text{m}$  to  $500\ \mu\text{m}$ .

Spring leaf was used for residual stress measurement. Upper part (see Fig. 1) was shot-peening treated and compressive residual stresses are expected, on other side the tensile residual stress should be present. Residual stress measurement was performed at room temperature in ambient conditions by X-ray diffraction method.

Piece of cut spring was used for residual stress measurement. Measurement was performed at shot-peening side of spring in longitudinal and transversal direction. Figure 4 shows the residual stress measurement by Stresstech Rollscan equipment. The measured compressive residual stress on the

surface was  $-493 \pm 20$  MPa in longitudinal direction. The similar value at the same depth was obtained by Scuracchio and co-workers [12]. The results of residual stresses showed that the maximum residual stress is obtained at a depth of about 0.25 mm and is about 1100-1200 MPa (in compression). It is significantly higher than the one near the surface. For higher depths the residual stress decreases and is in compression about -500 to -800 MPa at a depth of 0.35 mm. Regarding this measurement a residual stress equal to -1100 MPa will be considered for a depth equal to 0.25 mm and -500 MPa for 0.35 mm.

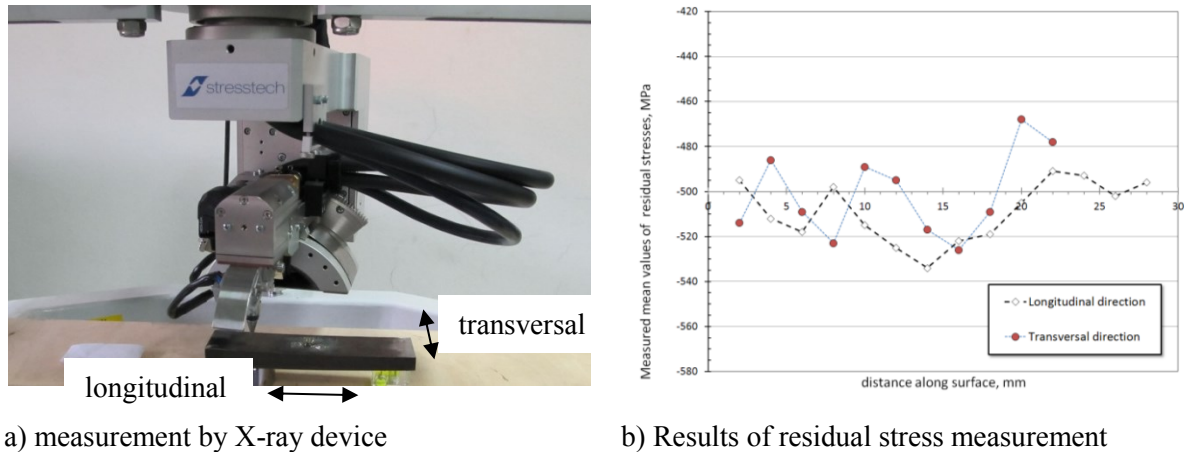


Fig. 5 Measurement of residual stresses at the polished point  $5\mu\text{m}$  under the surface

Murakami et al showed that the mechanism of fatigue failure starts around the inclusion as “Optical Dark Area” (ODA) as hydrogen embrittlement assisted by fatigue [13,14,15]. Murakami derived the model for the estimation of the threshold  $\Delta K_{th}$  as function of  $area^{1/2}$ :

$$\Delta K_{th} = 3.3 \cdot 10^{-3} \cdot (HV + 120) \cdot (\sqrt{area})^{1/3} \quad (4)$$

where  $HV$  is the Vickers hardness, in  $\text{kgf/mm}^2$ , and  $area^{1/2}$  is in  $\mu\text{m}$ , giving  $\Delta K_{th}$  in  $\text{MPa}\cdot\text{m}^{1/2}$ . The model works well till the  $\Delta K_{th}$  equals the threshold for long cracks. It seems that Murakami expression Eq. (4) works well till a value of  $area^{1/2}$  of 1 mm for low strength steel, where fatigue threshold equals the one for long crack. The value of  $area^{1/2}$  can be connected with inclusion size, as first iteration for initial fatigue crack length. Equation (4) shows also that the threshold for crack propagation increases with hardness. Therefore, it seems that with increasing of ODA and hardness of high strength material a higher fatigue threshold  $\Delta K_{th}$  value can be obtain. Unfortunately, docent of failures of springs steel are caused by different size of inclusions, from 0.1 until 1.5 mm diameter, where spring survived only few or couple of thousand cycles [10, 11].

However, Chapetti shows that opposite trend for fatigue threshold of long crack appear, as is shown in Fig. 6 [6]. For long cracks the threshold decreases with hardness [7], and becomes independent of crack length for a given  $R$  ratio. Chapetti shows that fatigue threshold vs. crack length exhibits bimodal behavior, one for short cracks and one for long cracks. Both models provide fatigue limit  $\Delta K_{th}$  as a function of crack length, but with Murakami’s model it is not possible to estimate fatigue life to failure. The pure fatigue crack propagation threshold for long cracks  $\Delta K_{th,R=-1}$  can be estimated by using the following empirical expression [7]:

$$\Delta K_{th,R=-1} = -0.0038 \cdot \sigma_u + 15.5 \quad (5)$$

Where the pure fatigue crack propagation threshold  $\Delta K_{th,R=-1}$  (a constant value for given tensile strength or hardness) are in  $\text{MPa}\cdot\text{m}^{1/2}$ , the crack length  $a$  in mm and the ultimate tensile strength  $\sigma_u$  in MPa.

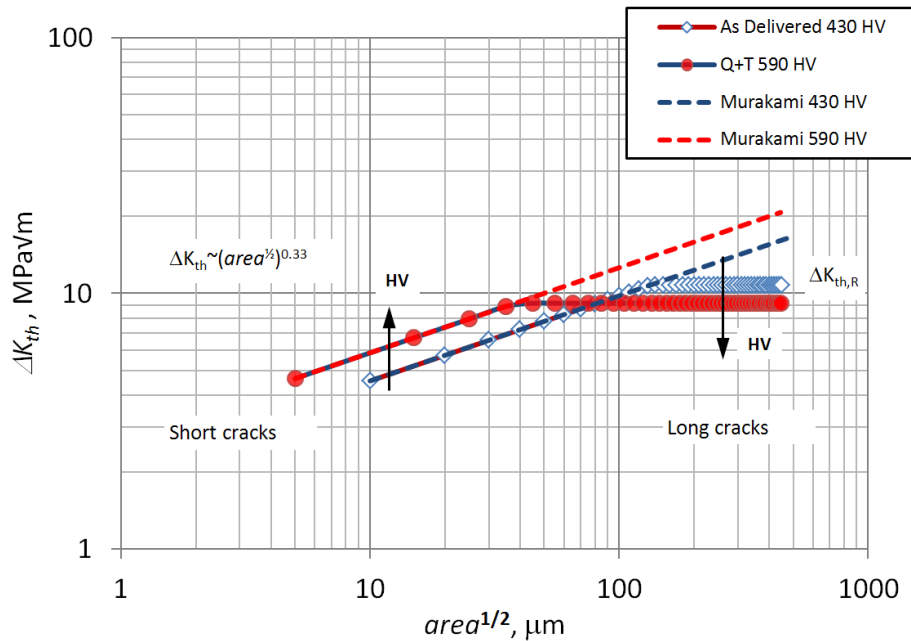


Fig. 6. Fatigue threshold as a function of  $area^{1/2}$  parameter for 51CrV4 steels: with hardness 430 HV as delivered and with hardness 590 HV in quenched and tempered condition

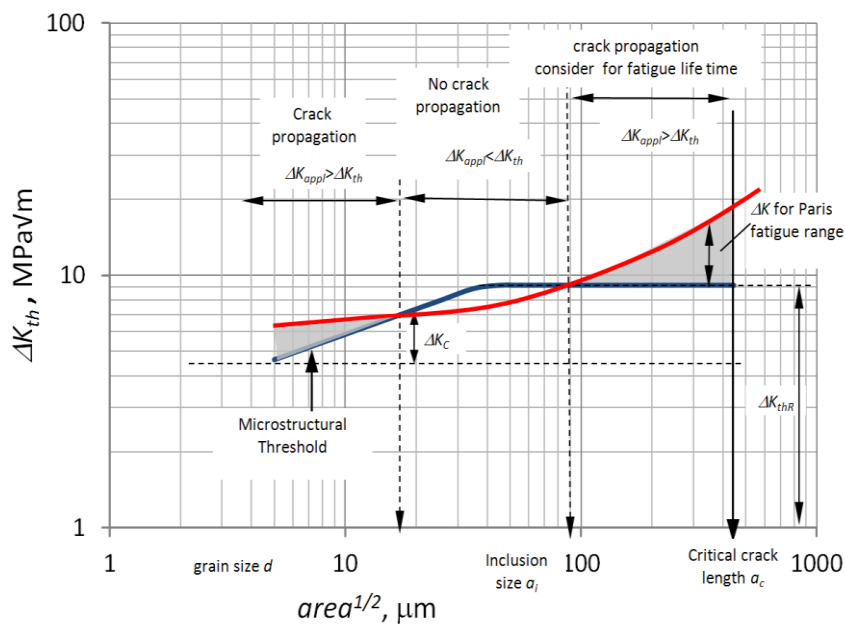


Fig. 7. Fatigue threshold as a function of  $area^{1/2}$  vs. fatigue crack driving force for short and long crack propagation

Figure 7 shows schematically by red line the fatigue crack driving force  $\Delta K$ . In the case of linear fracture mechanics and smooth specimens or spring after shot-peening, the following general expression can be used to estimate the applied driving force as a function of crack length [16]:

$$\Delta K = Y \cdot \Delta \sigma \sqrt{\pi \cdot a} \quad (6)$$

where  $\Delta \sigma$  is the stress range nominally applied at the initiation places.

The crack aspect ratio as a function of crack length has to be defined for the combination of component geometry and loading conditions, which allows definition of the value of the parameter  $Y$  as a function of crack length, same as in Eq. (1).

Therefore, if the fatigue crack's driving force  $\Delta K$  is lower than the fatigue threshold  $\Delta K_{th}$  respect to loading R ratio the fatigue crack does not grow.  $\Delta K_{th}$  depends also about loading R ratio. If the loading R ratio is smaller or even negative the  $\Delta K_{th}$  value is higher and fatigue crack will not grow.

A negative loading R ratio is possible to introduce by compressive residual stresses. Philosophy of leaf spring design is based on high strength of steel and induction of high compressive residual stresses in the tension loaded part of the spring. High strength steel grade 51CrV4 in thermo-mechanical treated condition is used for parabolic spring of heavy vehicles.

### 3. Fatigue Testing and Estimation of fatigue crack propagation life

Two groups of experimental results were obtained from representative specimens made from steel with hardness 590 HV in quenched and tempered condition. First group of tests are performed on hourglass specimens at room temperature using a four-axis cantilever type rotary bending fatigue machine at a stress ratio  $R=-1$ . Hourglass shaped specimens with a grip diameter of 15mm and minimum diameter of 7,5 mm were used. In order to induce minimum compress residual stress a specimens were grinded and electro-polishing in order to remove a layer of the surface about 10  $\mu$ m thick. In this set of specimens the residual stresses from surface are removed by electro-polishing.

Second group of specimens is single leaf of original spring for tracks. The tests were performed by spring producer as part of regular quality insurance of products. The springs are tested by bending with applied stress amplitude  $720 \pm 630$  MPa. Testing was performed in factory by frequency 1 Hz. This springs had residual stresses and were tested at a stress ratio  $R=90/1350=0.067$ .

Quantitative analysis of fatigue crack growth requires a constitutive relationship of general validity be established between the rate of fatigue crack growth,  $da/dN$ , and some function of the range of the applied stress intensity factor,  $\Delta K$  (crack driving force). Besides, it has to take into account the threshold for the whole crack length range, including the short crack regime where the fatigue crack propagation threshold is a function of crack length. Among others, the following relationship meets these requirements [7]

$$\frac{da}{dN} = C \cdot (\Delta K_{appl} - \Delta K_{th,R=-1})^m \quad (7)$$

where  $C$  and  $m$  are Paris range constants obtained from long crack fatigue behavior and  $\Delta K_{th,R=-1}$  is the crack growth threshold as lower value of Eq. (4) and (5). The fatigue crack propagation life from crack

initiation up to critical crack length  $a_c$  can be obtained by integrating expression (5) and using expression (4) for the threshold of the material ( $\Delta K_{th,R=-I}$ ). In the case of smooth specimens or spring after shot-peening, the stress can be considered constant for any crack length, equal to the nominal applied stress  $\Delta\sigma_n$ . The following general expression can be used to estimate the applied driving force as a function of crack length [8]:

$$\Delta K_{appl} = Y \cdot \Delta\sigma_n \sqrt{\pi \cdot a} \quad (8)$$

where  $\Delta\sigma_n$  is the nominal applied stress range.

The crack aspect ratio as a function of crack length has to be defined for the combination of component geometry and loading conditions, which allows definition of the value of the parameter  $Y=0.65$  [15] as a function of crack length, same as in Eq. (1).

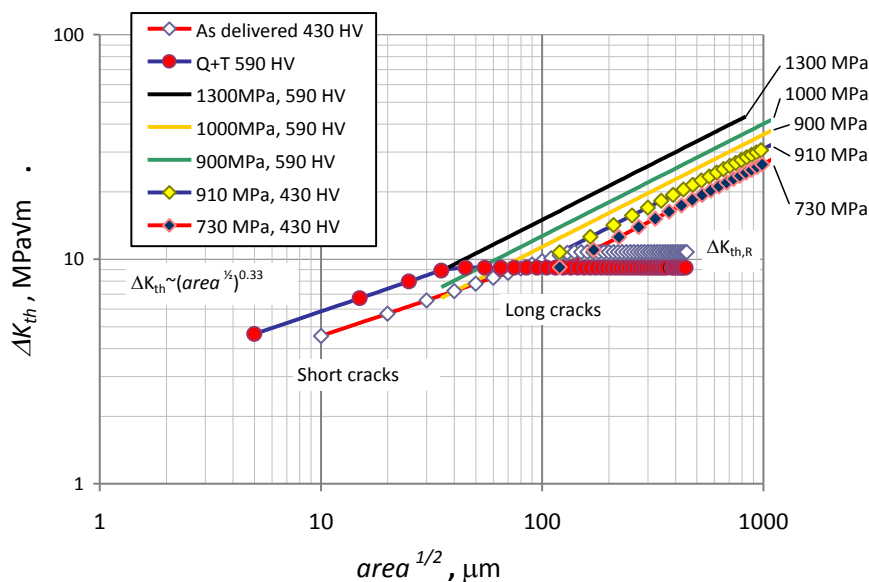


Fig. 8. Fatigue threshold as a function of  $area^{1/2}$  parameter for both conditions of steel

Figure 8 shows fatigue crack driving force as difference between applied force  $\Delta K_{appl}$  and threshold  $\Delta K_{th,R}$  obtained by Chapetti's model by applying Eq. (2). It is possible to determine the number of cycles to failure regarding to different inclusion size and different applied fatigue stress magnitude  $\Delta\sigma_n$ , by using simple integration of Eq. (7) with experimentally obtained parameters of Paris fatigue crack propagation range ( $C=8 \cdot 10^{-8}$  and  $m=3.25$ ). Fatigue crack propagation occur only if applied crack driving force  $\Delta K_{appl}$  is higher than threshold  $\Delta K_{th,R}$  and if inclusion size (as  $area^{1/2}$  in Fig. 8) is higher than value in intersection between threshold limit curve  $\Delta K_{th,R}$  and applied crack driving force line. Fatigue crack is going to propagate until critical crack length  $a_c$ . The value of critical crack length is determined by fracture toughness of material  $K_{IC}=33.19 \text{ MPa}\cdot\text{m}^{1/2}$ . Figure 8 shows fatigue crack driving force curves vs. initial crack area for constant applied stress  $\Delta\sigma_n$ . Figure 8 shows that as delivered steel (softer) switch to constant threshold value  $\Delta K_{th,R=-I}=10.769 \text{ MPa}\cdot\text{m}^{1/2}$  at larger size of inclusion  $a_i=120 \mu\text{m}$  than quenched and tempered steel, with size of inclusion  $a_i=35 \mu\text{m}$  and with constant threshold value  $\Delta K_{th,R=-I}=9.154 \text{ MPa}\cdot\text{m}^{1/2}$ .

Figure 9 shows results in form of  $S-N$  curves obtained by using proposed model for both conditions of 51CrV4 steel. Figure 9 shows the  $S-N$  curve obtained from hourglass specimens and points-results of

spring leaves testing made of steel in quenched and tempered (Q+T) conditions. The fatigue testing results of hourglass specimens are compared with model where initial crack corresponding to different inclusion's size e.g.  $a=0.15, 0.35$  and  $0.5$  mm. Different stress amplitudes  $\Delta\sigma_n$  under constant stress ratio  $R=-1$  and with constant inclusion size  $a$ , give a different number of cycles to failure. Obtained results as pairs of number of cycles  $N$  and applied stress amplitude  $\Delta\sigma_n$  at fixed inclusion size are connected to S-N curve. Model provides conservative values at lower number of cycles, lower than 50.000 and quite good agreement at higher number of cycles, at 100.000 cycles or more. Figure 9 shows that applied stress amplitude  $\Delta\sigma_n$  at same inclusion size (e.g.  $a=0.25$ mm) in case of compress residual stresses is few times higher at same number of cycles to failure. The results of spring leaves tests are in low cycle regime and all specimens shows subsurface inclusion-induced failure mode without Granular Bright Facets, as was mentioned in [10], and shown in Fig. 1.

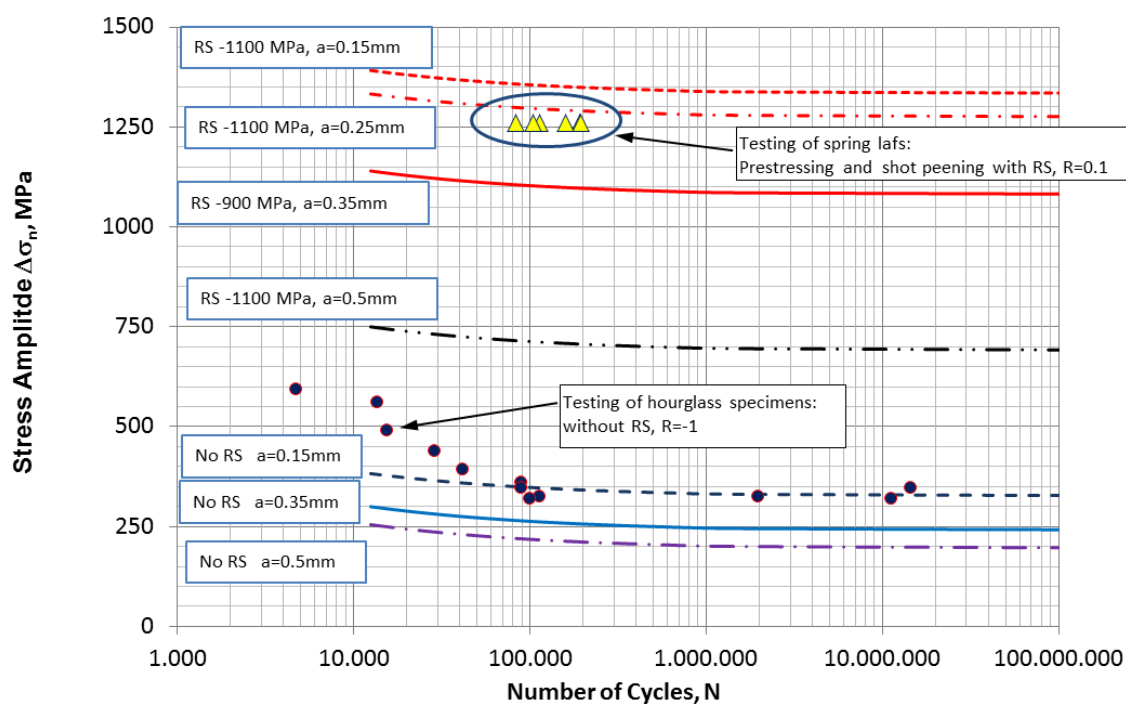


Fig. 9. Prediction of fatigue failure in form of S-N curve by using fracture mechanic approach and considering different size of inclusions in Q+T steel

Additional tests were conducted by spring producer on a leaf spring made from same steel with same inclusion size  $a_i = 0.5$  mm [10,11]. As it was mentioned the residual stresses on the surface should be at least  $\sigma_{RS} = -1100$  MPa. Tests were performed on six specimens. All six springs after pre-stressing and shot-peening were subjected the same loading regime ( $720 \pm 630$  MPa), therefore, an applied stress amplitude  $\Delta\sigma_n = 1260$  MPa and effective ratio  $R = (-1100 + 90) / (-1100 + 1350) = -4$ . The effective loading ratio  $R$  can vary, depending on inclusion distance from surface. The crack initiating inclusion, as is shown in Fig.1, lies 0.4 mm underneath the surface, in this region of crack initiation, the residual stresses are significantly lower!

All leaf springs failed between 80.000 and 195.000 number of cycles as shown in Fig. 8. The experimental results on specimen without residual stresses lie in the same range of cycles, but for an applied stress amplitude  $\Delta\sigma_n = 400$  MPa and ratio  $R = -1$ . Therefore, difference between thus two groups of experimental results is consequence of different  $R$  ratio, caused by residual stresses.

#### 4. Conclusions

Chapetti's model has been used for determination of a threshold  $\Delta K_{th}$  from short crack of grain size until critical crack length from less than one or only few millimeters corresponding to applied maximum stress  $\Delta\sigma_n/(1-R)$ . Life time of spring material subjected to applied stress amplitude  $\Delta\sigma_n$  from microstructural threshold up to critical crack length of high strength steel has been determined, by combining fracture mechanics parameters  $K_{IC}$ , fatigue propagation Paris range parameters  $C$  and  $m$ , and considering inclusion size  $a_i$  as crack initiation area. Results are presented in form of  $S-N$  curves. Approach shows good agreement with experimentally obtained fatigue results for spring steel in Q+T condition with same inclusion size.

Pre-stressing and shot-peening increase the magnitude of compressive residual stresses on the surface of the leaf spring, but for fatigue the inclusion-induction failure mode is relevant residual stress under the surface. Residual stresses change applied loading ratio  $R=90/1350=0.067$  to negative value  $R=-4$  under the surface.

Results also showed that the procedure allow as to analyze the different combinations of initial crack length and residual stress levels, and how much the fatigue resistance can change by changing that configuration. For this set of tests, the fatigue resistance estimated for an initial crack length equal to 0.35 mm, explain conservatively the high cycle fatigue, but it cannot be applied to estimate low cycles fatigue (high applied nominal stresses). The fatigue lives smaller than 50.000 cycles is associated to low cycle fatigue (LCF) and not to threshold conditions for fatigue crack propagation.

An integrated fracture mechanics approach is proposed to account for the estimation of the fatigue resistance of component. The model is simple to apply, accounts for the main geometrical mechanical and material parameters that define the fatigue resistance of the component and allows acceptable predictions.

It offers a change in design philosophy: It could be used for design, dealing with crack propagation thresholds. Besides, it allows to performed material defect sensitive analysis, quantified by fatigue lives and fatigue limit.

Acknowledgements:

Financial support by the Slovenian Research Agency (ARRS) and the Argentinean Ministry for Sciences in frame of bilateral project is gratefully acknowledged.

#### References

- [1] Shiozawa K, Lu L. Internal fatigue failure mechanism of high strength steels in gigacycle regime. *Key Eng Mat* 2008; 378-379:65-80.
- [2] Shiozawa K, Hasegawa T, Kashiwagi Y. Lu L. Very high cycle fatigue properties of bearing steel under axial loading condition. *Int J Fatigue* 2009;31:880-8.
- [3] Shimatani Y, Shiozawa K, Nakada T., Yoshimoto T., Effect of surface residual stress and inclusion size on fatigue failure mode of matrix HSS in very high cycle regime, *Procedia Engineering* 2010;2:873-882.
- [4] Tanaka K, Akiniwa Y. *Eng Fract Mech* 1988;30(6):863–76.
- [5] Chapetti MD. Fatigue propagation threshold of short cracks under constant amplitude Loading. *Int J Fatigue* 2003;25(12):1319–26.

- [6] M.D. Chapetti / *Engineering Fracture Mechanics* 75 (2008) 1854–1863
- [7] M.D. Chapetti / *International Journal of Fatigue* 33 (2011) 833–841
- [8] M.D. Chapetti, L.F. Jaureguizar. *Int J Fatigue* 43 (2012) 43–53
- [9] Black Almen, *Residual Stresses and Fatigue in Metals*, McGraw-Hill, New York, 1963
- [10] Gubeljak N. Predan J. Determination of dynamic strength of spring steel bellow yield stress, Industrial report for Štore Steel d.o.o. (in slovene), University of Maribor, Faculty of Mech. Eng. 2005
- [11] Štore Steel: Company report about testing of springs, by spring producer, Nov. 2008
- [12] B.G. Scuracchio, N. Batista de Lima, C.G. Schön. *Materials & Design*:47 (2013), 672-676.
- [13] Murakami Y, Nomoto T, Ueda T. *Fatigue Fract Eng Mater Struct* 1999;22:581–90.
- [14] Murakami Y, Nomoto T, Ueda T. *Fatigue Fract Eng Mater Struct* 2000;23:903–10.
- [15] Murakami Y, Nomoto T, Ueda T. *Fatigue Fract Eng Mater Struct* 2000;23:893–902.
- [16] H.O. Fuchs H.O. and Stephens R.I., *Metal Fatigue in Engineering*, John Wiley & Sons, New York, p. 130, 1980